Spin-flip scattering and critical currents in ballistic half-metallic *d*-wave Josephson junctions

Henrik Enoksen, Jacob Linder, and Asle Sudbø

Department of Physics, Norwegian University of Science and Technology, N-7491 Trondheim, Norway

We analyze the dc Josephson effect in a ballistic superconductor/half-metal/superconductor junction by means of the Bogoliubov–de Gennes equations. We study the role of spin-active interfaces and compare how different superconductor symmetries, including *d*-wave pairing, affect the Josephson current. We analyze the critical current as a function of junction width, temperature, and spin-flip strength and direction. In particular, we demonstrate that the temperature dependence of the supercurrent in the d_{xy} symmetry case differs qualitatively from the *s* and $d_{x^2-y^2}$ symmetries. Moreover, we have derived a general analytical expression for the Andreev bound-state energies that shows how one can either induce 0-π transitions or continuously change the ground-state phase of the junction by controlling the magnetic misalignment at the interfaces.

I. INTRODUCTION

The antagonistic nature of superconductivity and ferromagnetism makes their coexistence an unlikely one in bulk materials. In conventional superconductors, the current is carried by Cooper pairs consisting of two electrons in a spin singlet state, i.e., with antiparallel spins.[1] Ferromagnets on the other hand, favor parallel spin alignment. Hence one might expect that the proximity effect arising when bringing a ferromagnet into contact with a superconductor would decay rapidly due to this antagonistic nature.

However, it has been predicted that this rapid decay may not occur if there is some magnetic inhomogeneity present at the interface between a superconductor and a ferromagnet. Bergeret, Volkov, and Efetov[2] proposed a theory that coherent triplet Cooper pairs can be induced in ferromagnets, which in turn gives rise to a long-range triplet current. Several experiments have detected signs of this long-range triplet current,[3–7] and it is evident that a magnetic inhomogeneity is causing triplet pairing with parallel spins. Long-range triplet currents should also appear in inhomogeneous magnetic junctions with *d*-wave superconductors.[8]

Half metals[9] are fully spin-polarized ferromagnets, i.e., they are metallic for one spin direction and insulating for the other. Some half metals include CrO_2, $La_{0.7}Sr_{0.3}MnO_3$, and Fe_3O_4.[10] Keizer *et al.*[11] were the first to report long-range supercurrents through CrO_2. However, this group reported large variations in the magnitude of the critical current in the different samples. Moreover, some samples did not show any long-ranged supercurrent at all. Recent experiments have detected stable long-range currents believed to be caused by a formation of spin-triplet pairing.[12] All experiments report that some sort of spin-flip scattering caused by a magnetic inhomogeneity is required to obtain the long-range currents.

As there is only one spin direction at the Fermi level in half metals, the current passing through will be completely spin polarized. This has the potential for useful applications in low-temperature nanoelectronics. There have been several theoretical works on half-metallic Josephson junctions,[13–18] but to our knowledge no one has considered *d*-wave superconductors in this context. From a more general perspective, the interplay between unconventional superconductivity, such as *d*-wave pairing, and half metallicity has been studied in the context of magnetoresistance and spin-injection properties of cuprate/manganite hybrid structures.[19–22] The study of a half-metallic *d*-wave Josephson junction therefore has relevance for these types of materials.

In this paper, we will study how the supercurrent through unconventional half-metallic Josephson junctions depends on the properties of spin-active interfaces. We also study how the critical current depends on parameters like junction width and temperature for different levels of spin-flip scattering. Comparing the different superconducting symmetries, we find that a d_{xy}-wave superconductor gives a somewhat different result than *s*-wave and $d_{x^2-y^2}$ superconductors. Junctions made of half metals and the latter two types of superconducting order show a nonmonotonic temperature dependence of the critical current, while corresponding junctions involving d_{xy} superconductors do not show this behavior. Moreover, the junctions involving d_{xy} superconductors may sustain a critical current that is considerably larger than the two other superconducting symmetries. We also show that one can induce 0-π transitions[23] by switching the alignment of the magnetic interface fields from parallel to antiparallel. It is also possible to tune the ground-state superconducting phase by rotating the magnetic misalignment field at one interface relative to the other interface. These results are obtained numerically. We also provide a general analytical expression for the Andreev bound-state (ABS) energy spectrum that confirms our numerical findings.

The rest of the paper is organized as follows. In Sec. II, we introduce our model and notation. Our results are presented and discussed in Sec. III, and we present our conclusions in Sec. IV. We use ·$\hat{}$· for 4 × 4 matrices, and $\underline{\cdots}$ for 2 × 2 matrices. Boldface notation is used for three-vectors.

II. MODEL AND FORMALISM

We use a modified BTK (Blonder-Tinkham-Klapwijk) theory,[24] which takes into account arbitrary pairing symmetries and a spin-active S/F interface. We consider an S/F/S junction of width L; see Fig. 1 . The spin-active interfaces may induce long-range triplet currents. The propagation of quasiparticles is described by the Bogoliubov–de Gennes (BdG) equations

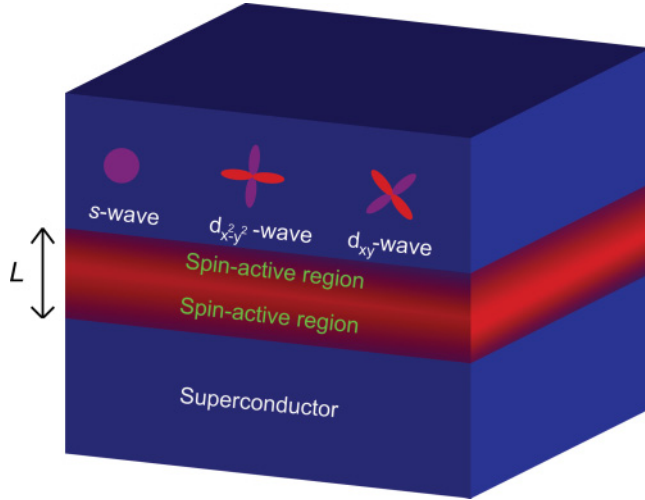$$\hat{H}\psi = \varepsilon\psi, \tag{1}$$

FIG. 1. (Color online) Schematic illustration of our system. A half metal of width L is sandwiched between two superconductors, which are considered as reservoirs. The superconductors may have either an s-wave or d-wave symmetry. The interface regions are assumed to be spin active due to, e.g., magnetic disorder or misaligned local magnetic moments.

where ψ is the eigenstate with energy eigenvalue ε. The Hamiltonian of the system is given by

$$\hat{H} = \begin{pmatrix} \underline{H_0} + \underline{V} & i\Delta(\theta)\underline{\sigma_2} \\ -i\Delta(\theta)^*\underline{\sigma_2} & -\underline{H_0} - \underline{V^*} \end{pmatrix}, \quad (2)$$

where

$$\underline{H_0} = \left(-\frac{\nabla^2}{2m} - E_F \right)\underline{\sigma_0} - h_z\Theta(x)\Theta(L-x)\underline{\sigma_3},$$

$$\underline{V} = \begin{pmatrix} V_\uparrow & V_x - iV_y \\ V_x + iV_y & V_\downarrow \end{pmatrix}[\delta(x) + \delta(x-L)]. \quad (3)$$

Here, $\Theta(x)$ and $\delta(x)$ denote the Heaviside step function and the δ function, respectively. The σ matrices are the Pauli matrices, m is the effective mass of the quasiparticles in both the superconductors and the ferromagnet and E_F is the Fermi energy. We assume equal Fermi energies in the different regions of the junction. The superconducting gap is denoted by $\Delta(\theta) = \Delta_0(T)g(\theta)[e^{i\varphi_L}\Theta(-x) + e^{i\varphi_R}\Theta(x-L)]$, where $g(\theta)$ accounts for the superconducting pairing symmetry, $\Delta_0(T)$ is the temperature-dependent gap amplitude, and $\varphi_{L(R)}$ is the phase of the left (right) superconductor. We consider the usual BCS temperature dependence $\Delta_0(T) = \Delta_0 \tanh(1.74\sqrt{T_c/T - 1})$ where T_c is the superconducting critical temperature. The exchange energy is h_z, and its direction is parallel to the z axis. We will consider the limit where the ferromagnet becomes half metallic, i.e., $h_z \to E_F$.

The barrier magnetic moment constitutes a spin-dependent potential $\underline{V}$, where the components entering Eq. (3) are given by

$$V_x = -\rho V_0 \cos\Psi \sin\phi,$$
$$V_y = -\rho V_0 \sin\Psi \sin\phi, \quad (4)$$
$$V_z = -\rho V_0 \cos\phi,$$

and $V_\sigma = V_0 + \sigma V_z$. $\sigma = \pm 1$ for spin up and spin down. See Fig. 2 for an illustration of the barrier magnetic moment and
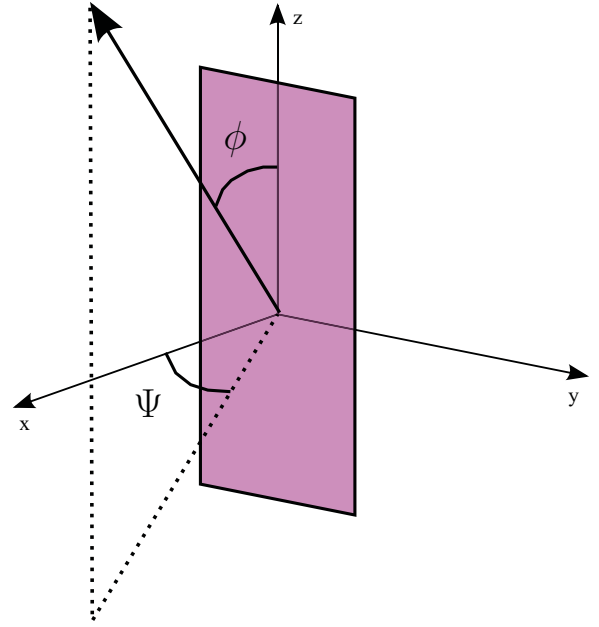

FIG. 2. (Color online) The barrier magnetic moment at the interface and its misalignment angles Ψ and ϕ. The bulk magnetization in the ferromagnet is assumed to be aligned with the z axis.

its misalignment angles Ψ and ϕ. The nonmagnetic barrier potential is V_0, while ρ is the ratio between the magnetic and nonmagnetic potentials, i.e.,

$$\rho = |\mathbf{V}|/V_0. \quad (5)$$

We assume that the bulk magnetization of the ferromagnet is aligned with the z axis in Fig. 2. For $\rho \neq 0$ with $\phi = 0$ we have spin mixing and with $\phi \neq 0$ we also have spin-flip. For details on spin mixing and spin-flip, see, e.g., Ref. 13.

Solving the BdG equations yields the wave function in the different regions of our system.[25] We can have four different incoming quasiparticles, electronlike quasiparticles (ELQs) with spin up and down, and holelike quasiparticles (HLQs) with spin up and down. For an incident spin-up electron in the left superconductor, the wave function is

$$\begin{aligned}\psi_L(x) &= [u_L(\theta_+),0,0,v_L(\theta_+)e^{-i\gamma_L^+}]e^{ik_+x} \\ &+ r_e^\uparrow[u_L(\theta_-),0,0,v_L(\theta_-)e^{-i\gamma_L^-}]e^{-ik_+x} \\ &+ r_e^\downarrow[0,u_L(\theta_-),\zeta v_L(\theta_-)e^{-i\gamma_L^-},0]e^{-ik_+x} \\ &+ r_h^\uparrow[0,\zeta v_L(\theta_+)e^{i\gamma_L^+},u_L(\theta_+),0]e^{ik_-x} \\ &+ r_h^\downarrow[v_L(\theta_+)e^{i\gamma_L^+},0,0,u_L(\theta_+)]e^{ik_-x}. \quad (6)\end{aligned}$$

For this particular process, the coefficients $r_e^\uparrow, r_e^\downarrow, r_h^\uparrow, r_h^\downarrow$ describe normal reflection, normal reflection with spin-flip, novel Andreev reflection, and usual Andreev reflection, respectively. We note that the momentum parallel to the interface is conserved for these processes.

The corresponding wave function in the right superconductor is

$$\begin{aligned}\psi_R(x) &= t_e^\uparrow[u_R(\theta_+)e^{i\varphi},0,0,v_R(\theta_+)e^{-i\gamma_R^+}]e^{iq_+x} \\ &+ t_e^\downarrow[0,u_R(\theta_+)e^{i\varphi},\zeta v_R(\theta_+)e^{-i\gamma_R^+},0]e^{iq_+x}\end{aligned}$$

$$+ t_h^\uparrow [0, \zeta v_R(\theta_-) e^{i\gamma_R^-} e^{i\varphi}, u_R(\theta_-), 0] e^{-iq_- x}$$
$$+ t_h^\downarrow [v_R(\theta_-) e^{i\gamma_R^-} e^{i\varphi}, 0, 0, u_R(\theta_-)] e^{-iq_- x}, \quad (7)$$

where the t's are the transmission coefficients, corresponding to the reflection processes described above. We have defined $e^{i\gamma_\pm} = \Delta(\theta_\pm)/|\Delta(\theta_\pm)|$ with $\theta_+ = \theta$ and $\theta_- = \pi - \theta$, and $\varphi = \varphi_R - \varphi_L$ is the phase difference over the junction. The parameter ζ accounts for singlet or triplet pairing in the superconductors. Here, we will consider only singlet pairing, i.e., $\zeta = -1$. Previous works have considered tunneling in p-wave superconductor/ferromagnet structures.[26–29] The coherence factors are defined as usual,

$$u(\theta) = \sqrt{\frac{1}{2}\left(1 + \frac{\sqrt{\varepsilon^2 - |\Delta(\theta)|^2}}{\varepsilon}\right)},$$

$$v(\theta) = \sqrt{\frac{1}{2}\left(1 - \frac{\sqrt{\varepsilon^2 - |\Delta(\theta)|^2}}{\varepsilon}\right)}. \quad (8)$$

$k_\pm = \sqrt{2m(E_F \pm \sqrt{\varepsilon^2 - |\Delta_L(\theta)|^2})}\cos\theta$ is the wave vector for ELQs (k_+) and HLQs (k_-) in the left superconductor and $q_\pm$ is the corresponding wave vector in the right superconductor. The wave function in the half metal is

$$\psi_{HM}(x) = (e e^{ik_e^\uparrow x} + f e^{-ik_e^\uparrow(x-L)})[1,0,0,0]$$
$$+ (e' e^{ik_e^\downarrow x} + f' e^{-ik_e^\downarrow(x-L)})[0,1,0,0]$$
$$+ (g e^{-ik_h^\uparrow x} + h e^{ik_h^\uparrow(x-L)})[0,0,1,0]$$
$$+ (g' e^{-ik_h^\downarrow x} + h' e^{ik_h^\downarrow(x-L)})[0,0,0,1], \quad (9)$$

where $k_{e,h}^\sigma = \sqrt{2m(E_F + \sigma h_z \pm \varepsilon)}\cos\theta$.

All scattering coefficients can be determined by matching wave functions at the interfaces. The boundary conditions are

$$\psi_L(0^-) = \psi_{HM}(0^+),$$
$$\partial_x[\psi_L(x) - \psi_{HM}(x)]|_{x=0} = 2m\underline{V_L}\psi_L(0) \quad (10)$$

for the left interface and

$$\psi_{HM}(L^-) = \psi_R(L^+),$$
$$\partial_x[\psi_{HM}(x) - \psi_R(x)]|_{x=L} = 2m\underline{V_R}\psi_R(L) \quad (11)$$

for the right. We will later use the parameter $Z = 2mV_0/k_F$ as a measure of interface transparency. Here, $k_F = \sqrt{2mE_F}$ is the Fermi wave vector. After the differentiation in the boundary conditions, we take the half-metallic limit $k_{e,h}^\downarrow \to 0$. From the boundary conditions we obtain a system of linear equations that yields the scattering coefficients.

With the scattering coefficients at hand, we can use a generalized version of the Furusaki-Tsukuda[18,30–32] formalism to calculate the Josephson current,

$$I(\varphi) = \frac{e}{4\beta} \sum_{\omega_n} \int_{-\pi/2}^{\pi/2} d\theta\, \Delta_L(\theta) \frac{k^+(\omega_n) + k^-(\omega_n)}{\Omega_n}$$
$$\times \left[\frac{a_1(\omega_n) - a_2(\omega_n)}{k^+(\omega_n)} + \frac{a_3(\omega_n) - a_4(\omega_n)}{k^-(\omega_n)}\right], \quad (12)$$

where $\omega_n = (2n+1)\pi/\beta$ are fermionic Matsubara frequencies with $n = 0, \pm1, \pm2, \ldots$, and $\Omega_n = \sqrt{\omega_n^2 + |\Delta_L(\theta)|^2}$. β is the inverse temperature. $k^+(\omega_n), k^-(\omega_n)$, and $a_i(\omega_n)$ are obtained from k^+, k^-, and a_i by analytically continuing ε to $i\omega_n$. a_i with $i = 1,2,3,4$ are the ordinary Andreev reflection coefficients for incoming ELQs with spin up or spin down, and incoming HLQ with spin up or spin down, respectively. The summation over the Matsubara frequencies is performed numerically.

If we neglect the contribution from the incoming quasiparticle, we get a homogeneous system of linear equations,

$$\Lambda x = 0, \quad (13)$$

where $x = [r_e^\uparrow, r_e^\downarrow, r_h^\uparrow, r_h^\downarrow, t_e^\uparrow, t_e^\downarrow, t_h^\uparrow, t_h^\downarrow]$ and Λ is an 8×8 matrix obtained by expressing the scattering coefficients in the half metal by the scattering coefficients in the left and right superconductor. By requiring a nontrivial solution of this system, $\det\Lambda = 0$, we find the Andreev bound-state energy spectrum E_i.

From the Andreev bound states we can find the Josephson current for a short junction $L/\xi \ll 1$, where ξ is the superconducting coherence length, in the ordinary way,[33]

$$I(\varphi) = 2e \sum_i \frac{\partial E_i}{\partial \varphi} f(E_i), \quad (14)$$

where e is the elementary charge and $f(E_i)$ denotes the Fermi-Dirac distribution function. We find the critical current from $I_c = \max_\varphi |I(\varphi)|$.

III. RESULTS

For conventional s-wave pairing we use $g(\theta) = 1$. For d wave we use $g(\theta) = \cos(2\theta - 2\alpha)$ where $\alpha = 0$ and $\pi/4$ correspond to $d_{x^2-y^2}$ and d_{xy} pairing, respectively. We will use the superconducting gap Δ_0 as a unit of energy. The Fermi energy is $E_F = 1000\Delta_0$, the interface transparency is $Z = 1$, and we use $T = 0.2T_c$ unless otherwise stated. We consider equal gap amplitude for the different pairing symmetries to ease the comparison. Unless otherwise stated, we assume that the magnetic misalignment angles ϕ and Ψ on both interfaces are equal.

Figure 3 shows the critical current for all three pairing symmetries for two values of ρ with misalignment angles $\phi = \pi/2$ and $\Psi = \pi/2$. The first value, $\rho = 0$, corresponds to no spin-flip. As expected, there is no current in this case. However, when spin-flip scattering is present, $\rho = 0.5$, we see that a long-range current appears. We find that junctions with s and $d_{x^2-y^2}$ symmetry behave very similarly, with $d_{x^2-y^2}$ having a slightly lower current magnitude. The critical current is proportional to the gap amplitude multiplied by a weighting factor depending on the Andreev reflection coefficients [see Eq. (12)] averaged over the angles of incidence θ. As the s-wave symmetry is independent of θ, its average is larger than for the $d_{x^2-y^2}$. The d_{xy} symmetry carries a current approximately three times larger than s and $d_{x^2-y^2}$ for our parameter choice.

Figure 4 shows how the critical current depends on the magnetic misalignment angle ϕ with $\Psi = \pi/2$ for three junction widths $kL = 10, 100, 1000$, which corresponds to widths of approximately 2, 20, and 200 nm, respectively. Notice that we obtain the maximal critical current at a misalignment angle
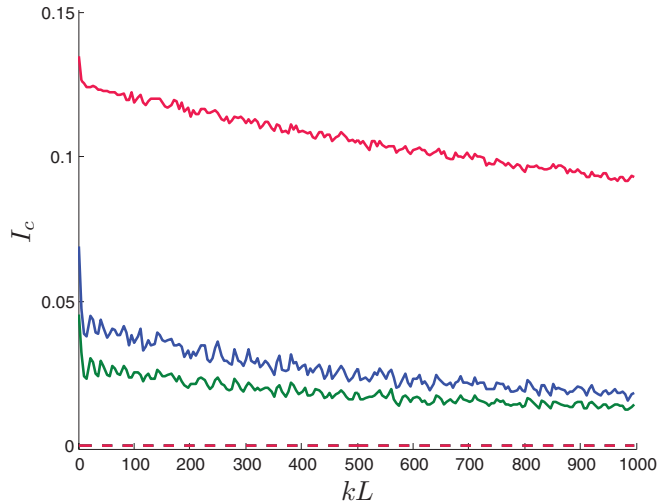
FIG. 3. (Color online) Critical current as a function of junction width for $\rho = 0$ (dashed lines) and $\rho = 0.5$ (solid lines) with misalignment angles $\Psi = \pi/2$ and $\phi = \pi/2$. Blue, green, and red lines indicate s-, $d_{x^2-y^2}$-, and d_{xy}-wave pairing symmetry, respectively.

FIG. 4. (Color online) Critical current as a function of the misalignment angle ϕ. Solid, dashed, and dash-dotted lines correspond to junction widths $kL = 10, 100$, and 1000, respectively. Panels (a)–(c) show s-, $d_{x^2-y^2}$-, and d_{xy}-wave pairing symmetry, respectively.

$\phi > \pi/2$ when the misalignment at both interfaces is parallel to each other. If we rotate the misalignment 180°, which is equivalent to inverting the exchange field $h_z \rightarrow -h_z$, the maximum will appear at $\phi < \pi/2$. As long as $h_z \neq 0$, the system is not invariant under a spatial inversion.[34] Therefore the direction of the exchange field relative to the misalignment field will determine whether the maximal current appears at misalignment angles smaller or larger than $\pi/2$.

If the magnetic moments at the interfaces are switched from parallel ($\rho_L = \rho_R$) to antiparallel alignment ($\rho_L = -\rho_R$), the current-phase relation changes sign as seen in Fig. 5 . This indicates a 0-π transition. Hence it is possible to induce 0-π transitions in half-metallic junctions by switching the relative direction between the two misalignment fields. Note that the other superconducting symmetries show the same behavior. We also note that for antiparallel alignment, the maximal critical current is obtained at a misalignment angle $\phi = \pi/2$ for both interfaces.

It is also possible to continuously change the ground-state phase of the junction by rotating the misalignment field at one interface relative to the other. Figure 6 shows the current-phase relation for a d_{xy} junction when the magnetic moment at the left interface points in the x direction while at the right interface the magnetic moment is rotated in the xy plane from being parallel to the left interface, to pointing in the y direction. Here, $\phi_L = \phi_R = \pi/2$. We see that the current changes continuously with Ψ_R. Hence, we can obtain a finite current at zero superconducting phase difference by tuning the magnetic misalignment fields. This is the same result as reported in Ref. 35 for s-wave superconductors. We get the same results for s- and $d_{x^2-y^2}$-wave junctions.

To gain further insight into the physical mechanisms underlying our numerical results, we have solved Eq. (13) analytically. This yields a rather large and complicated expression for the ABS energies, but it is nevertheless possible to infer how the interplay between the misalignment angles and superconducting phase difference is manifested. The resulting expression is

$$E = \pm |\Delta(\theta)| \sqrt{\frac{1}{2} + \frac{A_1 + A_2\tau\cos(\varphi + \chi) \pm \sqrt{B_1 + B_2\tau\cos(\varphi + \chi) + B_3\tau^2\cos^2(\varphi + \chi)}}{C}}, \tag{15}$$

where A_i, B_i, and C are large expressions that depend on junction parameters like junction width kL, the barrier magnetic moment $\mathbf{V}$, the angle of incidence θ, and the wave vectors $k_{e,h}^\uparrow$. $\tau = \alpha\rho^2 V_0^2 \sin^2\phi_L$ where $\alpha = \pm 1$ for parallel and antiparallel misalignment, respectively, and $\chi = \Psi_R - \Psi_L$ is the difference between the azimuthal angle of the right and left interface magnetic moments. As the Josephson current depends on the ABS energy differentiated with respect to φ, see Eq. (14), much of the qualitative behavior can be explained with this expression. First, if we have no spin-flip, i.e., $\phi = 0$ and/or $\rho = 0$, then $\tau = 0$. Every term containing
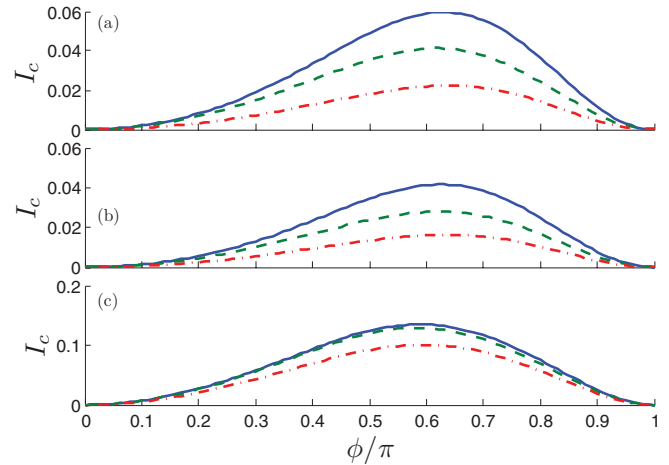
φ is multiplied by a τ factor, which shows that no spin-flip equals no current. This corresponds to the result we see in Fig. 3 where the current vanishes without spin-flip. Second, we see that a change of the magnetic misalignment on the two interfaces from parallel, $\alpha = 1$, to antiparallel $\alpha = -1$ is the same as shifting $\varphi \rightarrow \varphi + \pi$, i.e., a 0-$\pi$ transition like the one we see in Fig. 5. Last, the χ phase shows that it is possible to continuously change the ground-state phase of the junction by tuning the interface magnetic moments as shown in Fig. 6, since χ effectively renormalizes the superconducting phase difference: $\varphi \rightarrow \varphi + \chi$.
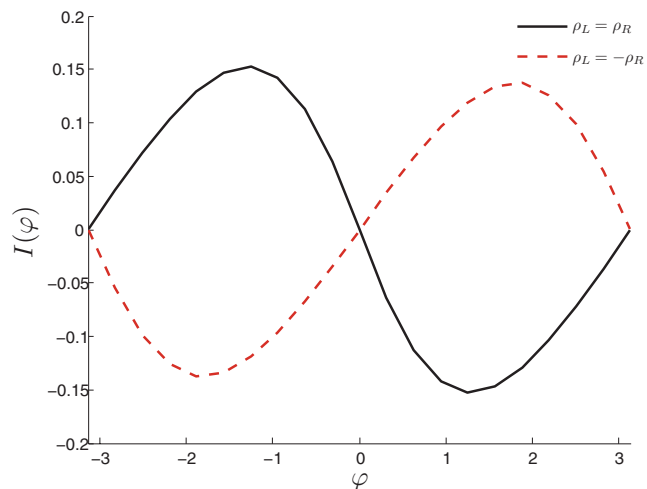
FIG. 5. (Color online) Current-phase relation for a junction with d_{xy} superconductors on both sides. The black solid line shows parallel misalignment at both interfaces, while the red dashed line shows antiparallel misalignment.

The most significant difference between the three gap symmetries is the temperature dependence of the critical current. The Josephson current in the case of d_{xy} symmetry decreases monotonically with increasing temperature, while the Josephson currents for the two other symmetries show a nonmonotonic behavior. Figure 7 demonstrates the temperature dependence of the critical current for the different gap symmetries.

This unusual temperature dependence can be explained by considering the proximity-induced density of states in the half metal. The critical current is proportional to the energy integral of the density of states multiplied by the slope of
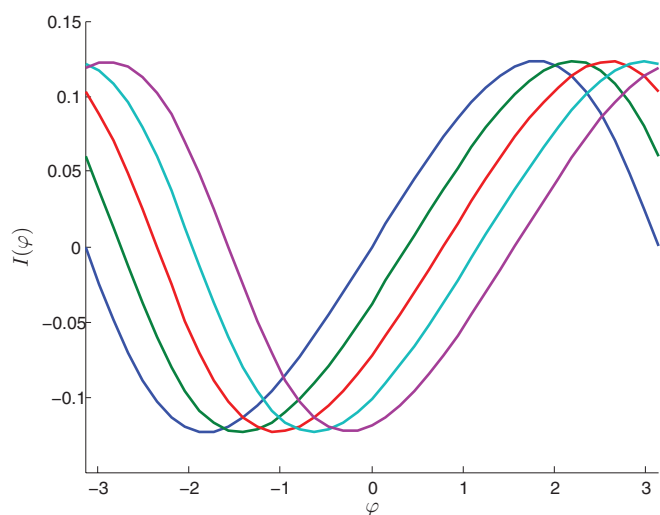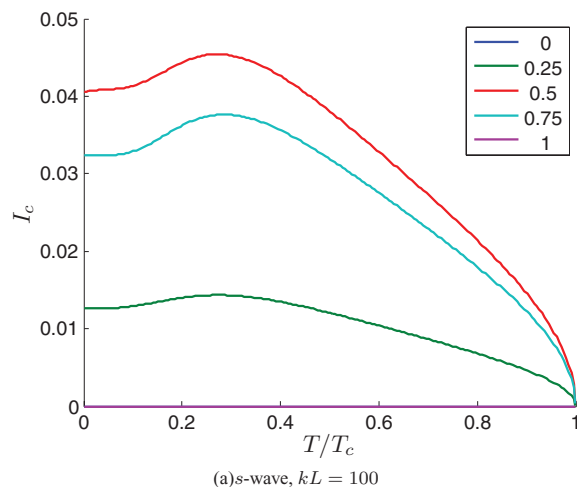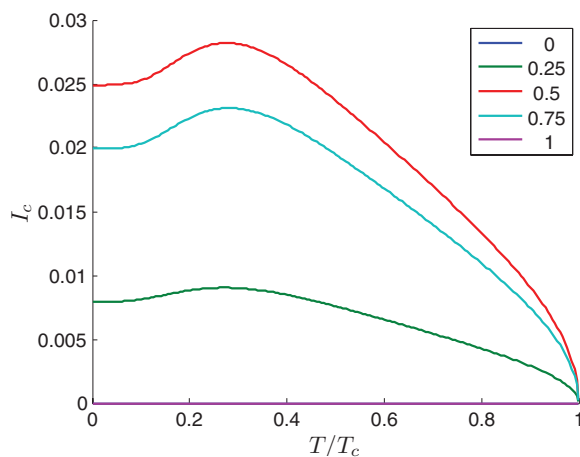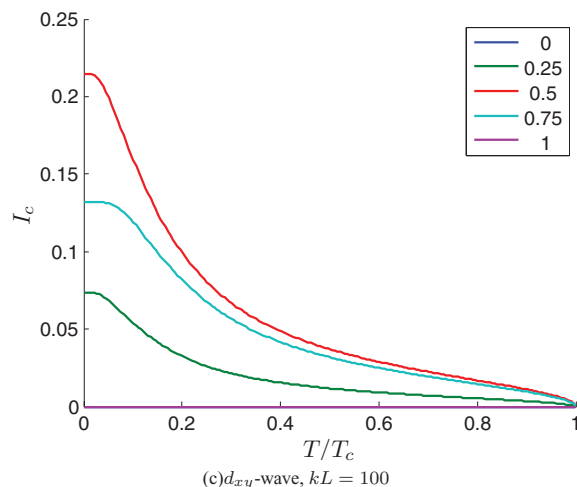

FIG. 6. (Color online) Current-phase relation for a junction with d_{xy} superconductors on both sides. The misalignment field in the xy plane is rotated from parallel to perpendicular, i.e., Ψ_R changes from 0 to $\pi/2$ in steps of $\pi/8$ (left to right). $\Psi_L = 0$ and $\rho_L = \rho_R = 0.5$. Here, $\phi_L = \phi_R = \pi/2$.

(a)s-wave, $kL = 100$

(b)$d_{x^2-y^2}$-wave, $kL = 100$

(c)d_{xy}-wave, $kL = 100$

FIG. 7. (Color online) Critical current as a function of temperature for all three superconducting symmetries at junction width $kL = 100$. Notice that the d_{xy}-symmetry decreases monotonically, while s- and $d_{x^2-y^2}$-symmetries have a non-monotonic behavior. The legends show the misalignment angle ϕ in units of π.

the Fermi distribution:[36]

$$I_c \sim \int dE\, N(E) \partial_E f(E), \qquad (16)$$

where $N(E)$ is a proximity-induced density of states in the half metal, which vanishes when superconductivity vanishes.

As shown in Refs. 36 and 37 the proximity-induced density of states for a half-metallic Josephson junction with s-wave superconductors has a peak at finite energies. Spin-flip processes at the interfaces create long-ranged spin-triplet pairs that penetrate the interface and create a peak in the density of states in the half metal due to the formation of bound states (in the ballistic limit). This peak is the origin of the nonmonotonic temperature behavior of the critical current that we also obtain; see Fig. 7(a). Subgap bound states may be thermally activated and contribute to the transport at a temperature T^* of the order of the energies of the bound states. Thus, when the temperature T is increased toward T^* the critical current can increase, although one should also take into account the fact that the superconducting order parameter is suppressed with increasing temperature. For the case of s-wave and $d_{x^2-y^2}$-wave superconducting gaps, the required temperature T^* is of the order of the gap amplitude. For a d_{xy}-symmetric gap, the bound states tend to be at lower energies close to the Fermi surface,[25] yielding a lower T^*, and hence a critical current that essentially is monotonically decreasing with temperature. We emphasize that all of this is contingent on the presence of spin-active tunneling barriers. Figure 7(b) shows that $d_{x^2-y^2}$ pairing yields the same nonmonotonic behavior as s-wave pairing, while Fig. 7(c) shows that d_{xy} pairing decays in the usual monotonic way.

We expect the same behavior for other superconducting symmetries as well: If the bound states are at energies close to the Fermi level, i.e., the density of states peaks at or very close to E_F, we expect the usual monotonic temperature dependence. However, if the bound states are at higher energies, i.e., the density of states peaks at higher subgap energies, we expect a nonmonotonic temperature dependence.

IV. CONCLUSIONS

In conclusion, we have analyzed the dc Josephson effect in an S/HM/S junction with spin-active interfaces. The possibility of spin-flip scattering at the interface creates equal spin triplet Cooper pairs in the half metal, such that a long-range supercurrent may be sustained. We have considered the role of unconventional superconducting symmetries, in particular d wave, and found that d_{xy} symmetry yields the largest critical current magnitude, while s and $d_{x^2-y^2}$ symmetry show similar behavior. In addition, the temperature dependence of the critical current is qualitatively different in the d_{xy}-wave case. Namely, while the current shows a nonmonotonic behavior for s and $d_{x^2-y^2}$ symmetry, it decays monotonically in the d_{xy}-wave case. This may be explained by considering the proximity-induced density of states in the half metal. When the density of states in the half metal has more weight near the Fermi level, as in the d_{xy}-wave case due to the hybridization of the bound states at the S/HM interfaces, the temperature dependence of the critical current is monotonically decaying as the temperature increases. On the other hand, if the density of states has a peak far from the Fermi level, we expect a nonmonotonic temperature dependence. We have also discussed how it is possible to switch between a 0 and π junction, both continuously and abruptly, by controlling the magnetic properties of the interfaces. Finally, we have found a general analytical expression for the Andreev bound-state energy spectrum, which confirms our numerical results.

[1] J. Bardeen, L. N. Copper, and J. R. Schrieffer, Phys. Rev. **108**, 1175 (1957); **106**, 162 (1957).

[2] F. S. Bergeret, A. F. Volkov, and K. B. Efetov, Phys. Rev. Lett. **86**, 4096 (2001).

[3] J. W. A. Robinson, J. D. S. Witt, and M. G. Blamire, Science **329**, 59 (2010).

[4] T. S. Khaire, M. A. Khasawneh, W. P. Pratt Jr., and N. O. Birge, Phys. Rev. Lett. **104**, 137002 (2010).

[5] J. Wang, M. Singh, M. Tian, N. Kumar, B. Liu, C. Shi, J. K. Jain, N. Samarth, T. E. Mallouk, and M. H. W. Chan, Nat. Phys. **6**, 389 (2010).

[6] I. Sosnin, H. Cho, V. T. Petrashov, and A. F. Volkov, Phys. Rev. Lett. **96**, 157002 (2006).

[7] D. Sprungmann, K. Westerholt, H. Zabel, M. Weides, and H. Kohlstedt, Phys. Rev. B **82**, 060505(R) (2010).

[8] A. F. Volkov and K. B. Efetov, Phys. Rev. Lett. **102**, 077002 (2009).

[9] W. E. Pickett and J. S. Moodera, Phys. Today **54**(5), 39 (2001).

[10] J. M. D. Coey and C. L. Chien, MRS Bull. **28**, 720 (2003).

[11] R. S. Keizer, S. T. B. Goennenwein, T. M. Klapwijk, G. Miao, G. Xiao, and A. Gupta, Nature (London) **439**, 825 (2006).

[12] M. S. Anwar, F. Czeschka, M. Hesselberth, M. Porcu, and J. Aarts, Phys. Rev. B **82**, 100501(R) (2010).

[13] M. Eschrig, J. Kopu, J. C. Cuevas, and G. Schön, Phys. Rev. Lett. **90**, 137003 (2003).

[14] Y. Asano, Y. Tanaka, and A. A. Golubov, Phys. Rev. Lett. **98**, 107002 (2007).

[15] M. Eschrig and T. Löfwander, Nat. Phys. **4**, 138 (2008).

[16] A. V. Galaktionov, M. S. Kalenkov, and A. D. Zaikin, Phys. Rev. B **77**, 094520 (2008).

[17] J. N. Kupferschmidt and P. W. Brouwer, Phys. Rev. B **83**, 014512 (2011).

[18] Z. M. Zheng and D. Y. Xing, J. Phys.: Condens. Matter **21**, 385703 (2009).

[19] G. Jakob, V. V. Moshchalkov, and Y. Bruynseraede, Appl. Phys. Lett. **66**, 2564 (1995).

[20] V. Pena, Z. Sefrioui, D. Arias, C. Leon, J. Santamaria, J. L. Martinez, S. G. E. te Velthuis, and A. Hoffmann, Phys. Rev. Lett. **94**, 057002 (2005).

[21] N. M. Nemes *et al.*, Phys. Rev. B **78**, 094515 (2008).

[22] J. Salafranca and S. Okamoto, Phys. Rev. Lett. **105**, 256804 (2010).

[23] V. V. Ryazanov, V. A. Oboznov, A. Yu. Rusanov, A. V. Veretennikov, A. A. Golubov, and J. Aarts, Phys. Rev. Lett. **86**, 2427 (2001).

[24] G. E. Blonder, M. Tinkham, and T. M. Klapwijk, Phys. Rev. B **25**, 4515 (1982).

[25] J. Linder, M. Cuoco, and A. Sudbø, Phys. Rev. B **81**, 174526 (2010).

[26] N. Stefanakis and R. Melin, J. Phys.: Condens. Matter **15**, 3401 (2003).

[27] J. Linder, M. S. Grønsleth, and A. Sudbø, Phys. Rev. B **75**, 054518 (2007).

[28] S. Wu and K. V. Samokhin, Phys. Rev. B **80**, 014516 (2009).

[29] P. M. R. Brydon, Y. Asano, and C. Timm, Phys. Rev. B **83**, 180504 (2011).

[30] A. Furusaki and M. Tsukuda, Solid State Commun. **78**, 299 (1991).

[31] Y. Tanaka and S. Kashiwaya, Phys. Rev. B **56**, 892 (1997).

[32] Y. Asano, Phys. Rev. B **64**, 224515 (2001).

[33] A. A. Golubov, M. Y. Kupriyanov, and E. Il'ichev, Rev. Mod. Phys. **76**, 411 (2004).

[34] J. Linder and A. Sudbø, Phys. Rev. B **82**, 020512(R) (2010).

[35] V. Braude and Yu. V. Nazarov, Phys. Rev. Lett. **98**, 077003 (2007).

[36] Y. Asano, T. Yokoyama, Y. Tanaka, and A. A. Golubov, Phys. Status Solidi A **205**, 1023 (2008).

[37] Y. Asano, Y. Sawa, Y. Tanaka, and A. A. Golubov, Phys. Rev. B **76**, 224525 (2007).